atmosphere

MDPI

Article

Incremental Evaluation Model for the Analysis of Indoor Air Measurements

Andreas Schmohl *, Michael Buschhaus, Victor Norrefeldt, Sabine Johann, Andrea Burdack-Freitag, Christian R. Scherer, Pablo A. Vega Garcia and Christoph Schwitalla

Fraunhofer Institute for Building Physics IBP, Fraunhoferstr. 10, 83626 Valley, Germany
* Correspondence: andreas.schmohl@ibp.fraunhofer.de; Tel.: +49-8024-643-205

Abstract: The investigation of the cleaning effectiveness of air cleaners under realistic conditions is challenging. Mathematical models are needed to extract characteristic properties of the air cleaning system from experimental data. An incremental evaluation model based on a source term and a total first-order loss coefficient in each segment was developed to analyze indoor particle measurements. The application of the model is demonstrated using two scenarios, one in a well-mixed testing room and another in a fully equipped aircraft cabin at 750 hPa with a typical aircraft ventilation system. In the first scenario, a normalized version of the model is used to eliminate the source's influence. For the investigation in the aircraft cabin, the model served to extract temporal and spatial resolved source terms and first-order loss coefficients. The incremental evaluation model is applicable to enhance the certification of air cleaners. The application of the model is not only limited to particles; measurements of gaseous compounds like ozone, carbon dioxide, or volatile organic compounds can be evaluated analogously. The model's utility for the data analysis of experiments with complex flow conditions should be studied in further investigations.

Keywords: mathematical model; data analysis; CADR; air purifier; air cleaner; aircraft cabin; particulate matter; spatial resolution; temporal resolution; curve fitting

Citation: Schmohl, A.; Buschhaus, M.; Norrefeldt, V.; Johann, S.; Burdack-Freitag, A.; Scherer, C.R.; Vega Garcia, P.A.; Schwitalla, C. Incremental Evaluation Model for the Analysis of Indoor Air Measurements. *Atmosphere* **2022**, *13*, 1655. https://doi.org/10.3390/atmos13101655

Academic Editor: Stefan Schumacher

Received: 30 August 2022
Accepted: 5 October 2022
Published: 11 October 2022

1. Introduction

Air cleaners (AC) can remove particulate matter (PM) and bioaerosols from indoor air [1–3]. The concept of a virtual clean air delivery rate (CADR) is used to specify the cleaning efficiency of an air cleaner at a certain physical volume flow [2–8]. The cleaning efficiency depends on the type of matter that has to be removed from the indoor air. The contaminants could be particulate matter [1–3,8,9], volatile organic compounds [10], or inorganic gaseous compounds. Furthermore, in the case of particulate matter, the cleaning efficiency of an air cleaner depends on the particle size distribution [2,3,6].

The removal effectiveness of an air cleaner can be specified in a laboratory under controlled and reproducible conditions. Mathematical models can implement the analysis of the experimental data of the test. Without a source that releases matter in the analyzed phase of the experiment, a simple exponential decay function can be used for the analysis [2,4–6]. While matter is released or contaminated outdoor air is infiltrating the room, a source term has to be considered [11–15]. Models based on a source term and a first-order loss term are common and well described elsewhere [3,8,10–12,14–18].

The general purpose of a fitting function is to describe a set of data. Ideally, all used fitting parameters are related to a physical-chemical meaning. The focus of this research was the development and application of an incremental fitting model. The model should be based on an equation that describes each segment. Hence for each phase of the experiment, the concentration curve between the concentration at the beginning of each segment and the equilibrium concentration at infinity. An analogous equation was utilized by Schumacher et al. and Jung; however, Jung did not use the option to string

together several segments to create an incremental evaluation model, and Schumacher et al. did not use the model for data analysis [3,12]. In the case of first-order kinetics, the equilibrium concentration in this model equals the source term divided by a first-order loss coefficient [3,12].

This research demonstrates the application of the incremental evaluation model using two scenarios. The first application scenario—"case study I"—is the determination of a clean air delivery rate (CADR) of a mobile air cleaner in a test room with well-mixed conditions. The second application scenario—"case study II"—investigates a non-thermal plasma air cleaning technology as an alternative technology for aircraft cabins. Generally, the feeding air in aircraft cabins is filtered by HEPA filters [9]. These filters are installed in the ventilation ducts. The advantage of the investigated alternative air cleaning technology was the reduction of the pressure drop in the ventilation duct resulting in lower energy consumption of the ventilation system. The flow conditions in aircraft cabins are complex; therefore, the temporal and spatial characteristics must be considered. When emitting particles in the aircraft cabin, measurements [19] and simulations [20] clearly show a spacial variation with increased concentrations closer to the emitter and lower concentrations farther away. This proves that the assumption of perfect mixing cannot be applied to such environments. Investigations in similar environments like train compartments similarly show that the distance from a virus emitter in the carriage is crucial for the exposure, and perfect mixing cannot be assumed [21,22]. Therefore, case study II focused on the temporal and spatial resolved evaluation of the source term s [$(\mu g/m^3)/h$)] and total first-order loss coefficient k [h^{-1}].

Applications of the incremental evaluation model for particulate matter, Phi6 bacteriophage bioaerosol, and ozone have recently been published [13,23].

2. Materials and Methods

2.1. Materials

Three identical light scattering aerosol spectrometers LSAS (Fidas Frog, Palas GmbH, Karlsruhe, Germany) were used to measure the aerosols in a micro range of 0.18–20 µm. The aerosol spectrometers continuously recorded PM fractions (PM_1, $PM_{2.5}$, and PM_{10}) and the particle number concentration.

A nebulizer (AGK 2000, Palas GmbH, Karlsruhe, Germany) nebulized an aerosol at 1.5 bar inlet pressure into the room air. The nebulized liquid was a Phi 6 (Pseudomonas Phage Phi6; DSM 21518) bacteriophage suspension, according to AHAM AC-5-2022 [24]. The molar concentrations of the salts in the suspension were: 86 mM NaCl, 49 mM Na_2HPO_4, 22 mM KH_2PO_4, 1 mM $CaCl_2$, and 1 mM $MgSO_4$.

The microbiological analysis is not relevant to this publication. However, microbiological sampling is described hereafter because the air sampling influenced the particle measurements (see Section 3.2.6). For the microbiological analysis, a bacteriophage plaque assay was used [23,25]. The plaque assay proceeded according to DIN EN 13610 [26]. Air samples for the plaque assays were collected with an airflow of 3 m^3/h by a Holbach air sampler (MBASS30V3, Umweltanalytik Holbach GmbH, Wadern, Germany).

2.2. Test Room for Determination of Clean Air Delivery Rate (CADR)

The air cleaner test was conducted in the Fraunhofer Indoor Air Test Center (IATC) in Valley, Germany (Figure 1). The IATC is a test facility with a room volume of 129 m^3 ($8.24 \times 5.06 \times 3.09$ m^3), where the climatic conditions are specifically set and kept constant over the measurement period. The test room was equipped with chairs and tables to simulate the situation in a classroom or an office.

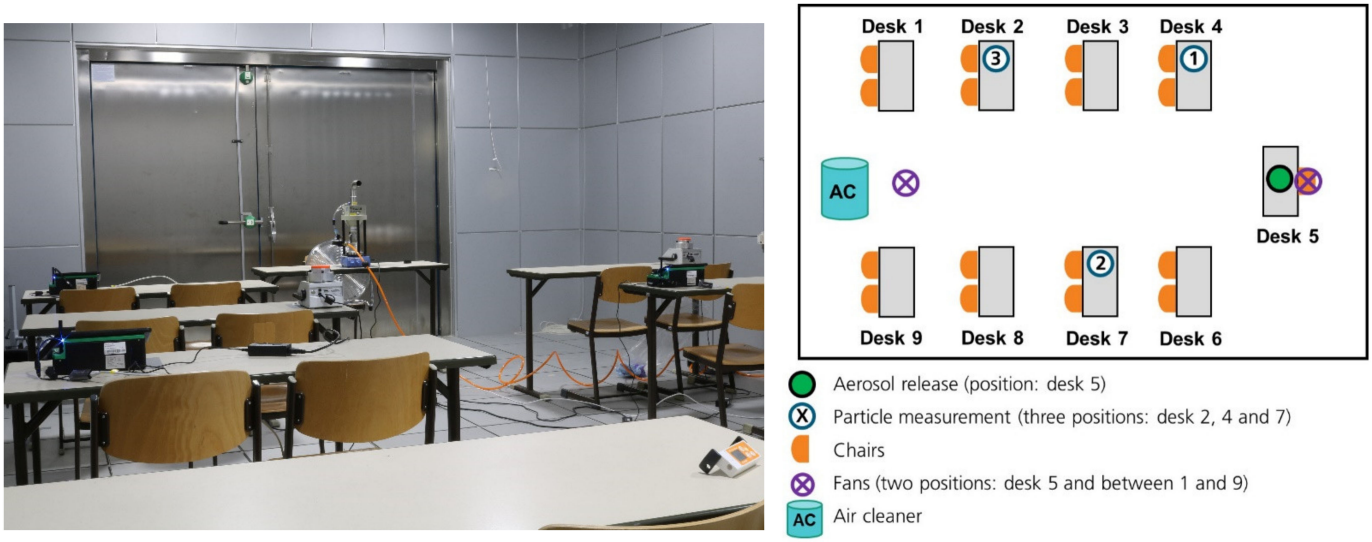

(**a**) (**b**)

Figure 1. IATC test setup with one aerosol generator, two fans, one air cleaner, and three particle measurement devices: (**a**) view towards aerosol generator; (**b**) positions of the aerosol generator, three particle counters, and the air cleaner (AC) in the test room.

The nebulizer continuously nebulized the phage suspension into the air. The aerosol spectrometers continuously recorded PM fractions in addition to the particle number concentration (or particle count, respectively) at three different positions in the room. Two fans, each with a volume flow of 400 m^3/h and directed against each other, mixed the air during the entire test procedure. One fan was placed behind the aerosol generator, and the second in front of the air cleaner (see Figure 1b). The test procedure was subdivided into five phases, see Table 1.

Table 1. Events during determining the clean air delivery rate of an air cleaner in a well-mixed test room.

Time of Day	t_{event} [h]	Event
11:30	−0.50	Start of particle measurement
12:00	0.00	Aerosol release was switched on.
13:00	1.00	Air cleaner with 100% power level was switched on.
14:00	2.00	Aerosol release was switched off.
14:40	2.67	Aerosol release was switched on and air cleaner reduced from 100% to 50% power level.
15:40	3.67	Aerosol release was switched off.
17:00	5.00	End of particle measurement

2.3. Investigation of an Air Cleaner in an Aircraft Cabin

The Fraunhofer Flight Test Facility (FTF) is a test platform on which aircraft ventilation systems and the tracing of in-cabin transmission can be investigated. In addition, real emission data can be used to evaluate various air cleaning devices. The full-size demonstrator consists of a front section of a long-range twin-aisle aircraft with ten rows of 2/4/2 seating (Figure 2). It has original ceiling air inlets, lateral inlets below the overhead bins, and extraction below the side wall at floor level into the triangle area (cheeks). Here the airflow is split into recirculation and exhaust air extracted from the bilge section. The aircraft's cabin volume is 107 m^3.

(**a**)

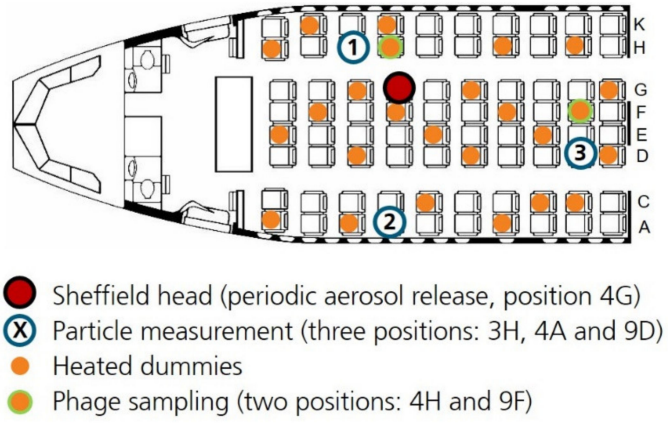

(**b**)

Figure 2. Aircraft cabin and positions: (**a**) interior view; (**b**) positions of the Sheffield head, three particle counters, two air samplers for phage plaque assay, and 25 heated dummies.

The experimental schedule and the documented events are listed in Table 2. The cleaning technology was implemented in the recirculation line. State of the art uses HEPA filters to purify the cabin air. In this test setup, the air in the recirculation line was first cleaned by a HEPA filter. Afterwards, the HEPA filter was removed and replaced by a non-thermal plasma air cleaner.

Table 2. Documented events during the investigation in the aircraft cabin.

Time of Day	t_{event} [min]	Event
08:00	−30	Ventilation with HEPA filter switched on
08:38	8	Start of particle measurement
09:17	47	Takeoff (pressure drop from 946 hPa to 750 hPa)
09:31	61	Cruising altitude reached (750 hPa)
09:32	62	Start of aerosol release (Sheffield head close to position 1)
10:30	120	Start of phage sampling
11:00	150	End of phage sampling
11:02	152	HEPA filter removed
11:13	163	Alternative technology on
12:13	223	Start of phage sampling
12:43	253	End of phage sampling
12:48	258	End of aerosol release
13:17	287	Descent (pressure rise from 750 hPa to 946 hPa)
13:21	291	Alternative technology off
13:34	304	Landing (946 hPa)
13:35	305	End of particle measurement

The experimental setup followed a scenario with a continuous emitter in the cabin, simulating the continuous exhalation of aerosols. The aerosol release was realized by a modified "breathing" Sheffield head which was combined with the aerosol generator and placed at seat number 4G (black head in Figure 2a) [27]. The modified head was "breathing" 20 cycles per minute with 2 L "respiratory volume" per cycle resulting in an output of 40 L/min or 2.4 m^3/h, respectively. The aerosol spectrometers continuously recorded the PM fractions and the particle number concentration at three positions (3H, 4A, and 9D; see Figure 2b). For the evaluation, the $PM_{2.5}$ fraction was used.

Indoor climate parameters were set to 23 °C, 5–15% relative humidity, and 750 hPa. This pressure is typical for cruise conditions. The aircraft ventilation system provided an airflow of 846 m^3/h, of which 50% was fresh air and 50% was recirculated air. The total

airflow corresponds to a mean air exchange rate of 7.9 h^{-1}. The airflow in the cabin was 63% ceiling outlet and 37% below the overhead bins. The ventilation nozzles were not used. A total of 25 passengers were simulated by 25 heated dummies (75 W, human-like shape). Each passenger received 34 m^3/h of cabin air.

2.4. Mathematical Basics

2.4.1. Clean Air Delivery Rate

The clean air delivery rate (CADR) is the virtual volume flow of clean air [m^3/h] supplied by an air cleaner. While the experimentally determined loss coefficient k_{AC} is characteristic for the test setup, the CADR is characteristic for the air cleaner itself [2,4–7]. The loss coefficient k_{AC} of the air cleaner is the total loss coefficient k minus the natural loss coefficient k_{nat}, which describes the behavior of the test setup without an air cleaner.

The clean air delivery rate of an air cleaner [2–8] is the product of the loss coefficient due to the air cleaner and the room volume, see Equation (1):

$$\text{CADR} = k_{AC} \times V = (k - k_{nat}) \times V \quad (1)$$

where CADR is the clean air delivery rate in [m^3/h], k_{AC} is the air cleaner loss coefficient in [h^{-1}], k_{nat} is the natural loss coefficient in [h^{-1}], k is the total loss coefficient in [h^{-1}], and V is the room volume in [m^3].

Volume V is the volume in which the locally determined total loss coefficient k and the natural loss coefficient k_{nat} are valid. Hence, a necessary condition for determining a CADR is to have well-mixed conditions in the room. Otherwise, neither the volume V nor the time-resolved natural loss coefficient k_{nat} are known. Therefore, a homogeneous concentration in the whole room is mandatory.

2.4.2. Steady State Condition

In a steady state condition, the source term s [µg/(m^3 h] equals the concentration loss [µg/(m^3 h]. In the case of first-order kinetics, the concentration loss in the steady state is the product of the equilibrium concentration and the total first-order loss coefficient [h^{-1}]. The steady-state condition is expressed by Equation (2):

$$s = c_{eq} \times k \quad (2)$$

where s is the source term in [µg/(m^3 h)], c_{eq} is the equilibrium concentration in [µg/m^3], and k is the total loss coefficient in [h^{-1}].

There can be several contributions to the source term s. Equation (3) represents an example for a source term s:

$$s = R/V + c_{in} \times F/V \quad (3)$$

where s is the source term in [µg/(m^3 h)], R is the release rate in [µg/h], V is the room volume in [m^3], c_{in} is the concentration in [µg/m^3] in the outdoor air infiltrating the room, and F is the flow in [m^3/h] streaming into volume V.

The total first-order loss coefficient k can be considered a sum of first-order loss processes. Equation (4) represents an example of a total first-order loss coefficient k:

$$k = \left(k_{sed} + k_{react} + k_{aglom} + F/V\right) \quad (4)$$

where k is the total loss coefficient in [h^{-1}], k_{sed} is the loss coefficient due to sedimentation in [h^{-1}], k_{react} is the loss coefficient due to reactions in [h^{-1}], and k_{aglom} is the loss coefficient due to agglomeration in [h^{-1}]. The volume flow F in [m^3/h] divided by volume V in [m^3] results in the air exchange in [h^{-1}].

While the determination of a CADR needs well-mixed conditions, the spatially resolved determination of a loss coefficient k can be used without this requirement.

3. Results

An incremental model consists of various calculation segments. Each segment represents a characteristic part of the concentration curve and corresponds to a phase of the analyzed experiment. The basis of this work was the development of an equation describing the concentration curve between the concentration at the beginning of each segment and the equilibrium concentration at infinity. As the concentration converges to a steady state, this equation can be called a steady state convergence function.

The concentration at a certain time can be described by Equation (5):

$$c_n(t) = c_{eq,n} + \left(c_{n-1}(t_{n-1}) - c_{eq,n}\right) \times e^{-k_n \times (t - t_{n-1})} \quad (5)$$

where $c_n(t)$ is the concentration in [µg/m^3] at a certain time t in [h], $c_{eq,n}$ is the equilibrium concentration in [µg/m^3] of phase n, $c_{n-1}(t_{n-1})$ is the concentration in [µg/m^3] at the beginning of phase n at t_{n-1} in [h], and k_n is the total first-order loss coefficient in [h^{-1}] of phase n.

With $t = t_{n-1}$, Equation (5) results in the initial concentration c_{n-1}. The outcome for t towards infinity is the equilibrium concentration c_{eq}. The concentration curve between the initial and final concentration is described by an e-function.

The final concentration of phase n is not necessarily the equilibrium concentration. The concentration c_n at the end of phase n is calculated by Equation (6) analogous to Equation (5) by using the time parameter t_n of the end of phase n:

$$c_n = c_n(t_n) = c_{eq,n} + \left(c_{n-1} - c_{eq,n}\right) \times e^{-k_n \times (t_n - t_{n-1})} \quad (6)$$

The concentration at the beginning of a certain phase n is equal to the concentration at the end of the previous phase $n-1$ at t_{n-1}. At the beginning of the first phase ($n = 1$), the concentration $c_{n-1}(t_{n-1})$ is $c_0(t_0)$.

3.1. Case Study I: Determination of a Clean Air Delivery Rate under Well Mixed Conditions

3.1.1. Fitting Function

Typically, the testing of air cleaners is implemented under controlled conditions and with a fixed testing procedure. At the beginning of the test (phase zero), there is an initial period with no aerosol release and no active air cleaner. The concentration c_0 at the beginning of the test should be small enough to be neglectable.

At the beginning of the first phase, the source was switched on ($r = 1$) while the air cleaner stayed off (power level $p = 0\%$). The concentration c_1 at the end of phase 1 was used to normalize; see Equation (5). For the normalized function $f_n(t)$, the parameter s_n was replaced by the product of the normalization parameter N with the parameter r that characterizes the status of the source. The result of this normalization process was Equation (7):

$$f_n(t) = \frac{N \times r_n}{k_n} + \left(f_{n-1} - \frac{N \times r_n}{k_n}\right) \times e^{-k_n \times (t - t_{n-1})} \quad (7)$$

$$\text{with } N = k_{nat} / \left[1 - e^{-k_{nat} \times (t_1 - t_0)}\right]$$

where $f_n(t)$ is the normalized concentration [-] at a certain time t in [h] during phase n, N is a normalization parameter [h^{-1}], k_n is the total loss coefficient in [h^{-1}] in phase n, k_{nat} is the natural loss coefficient in [h^{-1}] determined in phase 1, t_0 is the time in [h] at the beginning of the aerosol release, t_1 is the time in [h] at the beginning of the simultaneous operation of aerosol release and air cleaner, t_{n-1} is the time in [h] at the beginning of phase n, f_{n-1} is the normalized concentration [-] at the end of the previous phase $n-1$ at t_{n-1}, and r_n is a parameter that characterizes the status of the source: $r = 0$ means off and $r = 1$ means on.

The value f_n at the end of phase n ($t = t_n$) was calculated by Equation (8), analogous to Equation (7):

$$f_n = f_n(t_n) = \frac{N \times r_n}{k_n} + \left(f_{n-1} - \frac{N \times r_n}{k_n}\right) \times e^{-k_n \times (t_n - t_{n-1})} \quad (8)$$

The total loss coefficient k_n for a certain phase n was calculated by Equation (9):

$$k_n = k_{nat} + p_n \times e_{p,n} \times k_{AC} \quad (9)$$

where k_n is the total loss coefficient in [h^{-1}] in phase n, k_{nat} is the natural loss coefficient in [h^{-1}] determined in phase 1, p_n is the power level (between 0 and 100%) of the air cleaner, $e_{p,n}$ is the efficiency of the air cleaner at a certain power level p (e.g., $e_{50\%}$ at 50% power level in Table 3), and k_{AC} is the loss coefficient in [h^{-1}] due to the air cleaner.

Table 3. Resulting set of equations for the five segments of the incremental model.

Phase n *	**Start** t_{n-1}	**End** t_n	$f_n(t)$ **with** $N = k_{nat}/[1 - \exp[-k_{nat} \times (t_1 - t_0)]]$		
n	t_{n-1}	t_n	$f_n(t) = N \times r_n/k_n + (f_{n-1} - N \times r_n/k_n) \times \exp[-k_n \times (t - t_{n-1})]$	with	$k_n = k_{nat} + p_n \times e_n \times k_{AC}$
1	0	1.00	$f_1(t) = N \times 1/k_1 + (0 - N \times 1/k_1) \times \exp[-k_1 \times (t - 0)]$	with	$k_1 = k_{nat} + 0 \times 0 \times k_{AC}$
2	1.00	2.00	$f_2(t) = N \times 1/k_2 + (1 - N \times 1/k_2) \times \exp[-k_2 \times (t - 1.00)]$	with	$k_2 = k_{nat} + 1 \times 1 \times k_{AC}$
3	2.00	2.67	$f_3(t) = N \times 0/k_3 + (f_2(t_2) - N \times 0/k_3) \times \exp[-k_3 \times (t - 2.00)]$	with	$k_3 = k_{nat} + 1 \times 1 \times k_{AC}$
4	2.67	3.67	$f_4(t) = N \times 1/k_4 + (f_3(t_3) - N \times 1/k_4) \times \exp[-k_4 \times (t - 2.67)]$	with	$k_4 = k_{nat} + 0.5 \times e_{50\%} \times k_{AC}$
5	3.67	5.00	$f_5(t) = N \times 0/k_5 + (f_4(t_4) - N \times 0/k_5) \times \exp[-k_5 \times (t - 3.67)]$	with	$k_5 = k_{nat} + 0.5 \times e_{50\%} \times k_{AC}$

* The fitted curve was divided in five segments with known or defined parameters t_{n-1}, f_0, f_1, r_n, p_n, $e_{0\%} = 0$, $e_{100\%} = 1$ and three unknown variables k_{nat}, k_{AC} and $e_{50\%}$.

3.1.2. Fitting Process

Initially, the fitting model was constructed by setting up five equations analogous to the normalized Equation (7) for five phases ($n = 1$ up to $n = 5$) and by including the known parameters in these five equations (Table 3).

The mean values for PM_{10}, $PM_{2.5}$, and PM_1 and the particle count from the particle measurement at three positions in the test room were each calculated and normalized by the maximum concentration at the end of phase 1. The maximum $PM_{2.5}$ concentration reached 517 µg/m^3 at maximum after 1 h aerosol release. The relative standard deviation of $PM_{2.5}$ at the three positions did not exceed 12% (or <12 µg/m^3 for <100 µg/m^3). The $PM_{2.5}$ concentration in the initial phase (phase 0) was 2.1 ± 0.9 µg/m^3, thus only 0.4% of the maximum concentration.

The resulting total fitting curve (Table 3) can be divided into 3 parts. The first part ($n = 1$) was used to adjust k_{nat}, the second ($n = 2$ and 3) to adjust k_{AC}, and the third ($n = 4$ and 5) to adjust $e_{50\%}$. Therefore the fitting process was done in three steps:

1. The parameter k_{nat} was changed until the curvature of the curve $f_1(t)$ met the experimental data in phase 1. The parameter t_1 was adjusted slightly;
2. The parameter k_{AC} was changed until the curve met the experimental data in phases 2 and 3. The parameters t_2 and t_3 were adjusted slightly;
3. The parameter $e_{50\%}$ was changed until the curve met the experimental data in phases 4 and 5. The parameters t_4 and t_5 were adjusted slightly.

3.1.3. Fitting Results

The results of the fitting process are shown in Table 4 and Figure 3. Notice that the curve of the normalized concentration can be described for 5 h and 5 different testing modes (parameters changed: 3 power levels of AC and release on/off) very well (variance between 5% and 10%) with only three unknown variables (k_{nat}, k_{AC}, and efficiency $e_{50\%}$). Until 2.68 h (phases 1, 2, and 3), only two variables (k_{nat} and k_{AC}) were necessary.

Table 4. Known parameters t_{n-1}, p_n, and r, and variable fitting parameters k_{nat}, $k_{AC,}$ and $e_{50\%}$ for the fitting curve in Figure 3.

Phase n * [-]	t_{n-1} (Start) [h]	k_{nat} [h^{-1}]	k_{AC} [h^{-1}]	AC Power Level p	AC Efficiency e	Release r	k_n [h^{-1}]	$f_{start,n}$ [-]	$f_{eq,n}$ [-]
1	0.00	**0.5**	**3.0**	0% (off)	-	1 (on)	0.5	0.00	2.51
2	1.02	**0.5**	**3.0**	100% (on)	$e_{100\%} = 1$	1 (on)	3.5	1.00	0.36
3	2.02	**0.5**	**3.0**	100% (on)	$e_{100\%} = 1$	0 (off)	3.5	0.38	0.00
4	2.68	**0.5**	**3.0**	50% (on)	$e_{50\%} =$ **1.14**	1 (on)	2.21	0.04	0.57
5	3.68	**0.5**	**3.0**	50% (on)	$e_{50\%} =$ **1.14**	0 (off)	2.21	0.52	0.00

* The fitted curve was divided into five model segments with individual parameters p, e, and r. The fitting parameters k_{nat} and k_{AC} have been kept constant for all five segments. Bold type numbers are unknown variables used for matching the curve to the measurement data.

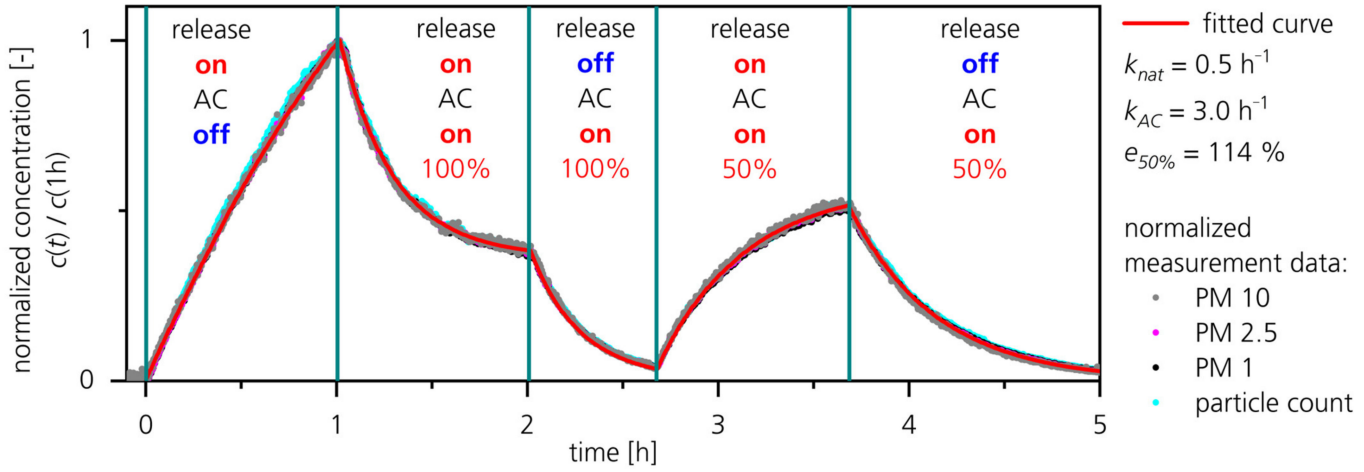

Figure 3. Determination of the coefficient k_{AC} of an air cleaner (AC) in a well-mixed room. The natural loss coefficient is determined between 0 and 1 h. (Fitting process see Section 3.1.2.).

The clean air delivery rate (CADR) is calculated subsequently by Equation (10):

$$\text{CADR} = k_{AC} \times V = 3.0\,\text{h}^{-1} \times 129\,m^3 = 387\,m^3/\text{h} \quad (10)$$

where CADR is the clean air delivery rate in [m^3/h], k_{AC} is the air cleaner loss coefficient in [h^{-1}], and V is the volume of the test room in [m^3].

At 50% power level the efficiency e of the air cleaner was higher ($e_{50\%}$ = 114%) than at 100% power level ($e_{100\%}$ is defined as 100%).

3.2. Case Study II: Investigation of an Air Cleaner in an Aircraft Cabin

3.2.1. General Aspects concerning the Fitting Model

The equilibrium concentration of a certain phase was calculated by Equation (11):

$$c_{eq,n} = \frac{s_n}{k_n} \quad (11)$$

where $c_{eq,n}$ is the equilibrium concentration in [µg/m^3] in phase n, s_n is the source term in [µg/(m^3 h] in phase n, and k_n is the total loss coefficient in [h^{-1}] in phase n.

The source term s at a certain location was not the same as the release rate of the particle source because only a part of the released particles flowed through the volume compartment where the measurement took place.

The concentration at a certain time was calculated by Equation (12):

$$c_n(t) = \frac{s_n}{k_n} + \left(c_{n-1}(t_{n-1}) - \frac{s_n}{k_n}\right) \times e^{-k_n \times (t - t_{n-1})} \quad (12)$$

where $c_n(t)$ is the concentration in [µg/m^3] at a certain time t in [h] during phase n, s_n is the source term in [µg/(m^3 h] in phase n, k_n is the total loss coefficient in [h^{-1}] in phase n, and $c_{n-1}(t_{n-1})$ is the concentration in [µg/m^3] at the end of the previous phase $n-1$ at t_{n-1} in [h].

The concentration c_n at the end of phase n was calculated by Equation (13), analogous to Equation (12):

$$c_n = c_n(t_n) = \frac{s_n}{k_n} + \left(c_{n-1} - \frac{s_n}{k_n}\right) \times e^{-k_n \times (t_n - t_{n-1})} \quad (13)$$

The parameter k_n affects the curvature of the fitted curve. Both parameters together affect the concentration level. As the curvature of the curve is only influenced by parameter k_n, the curvature of the fitted curve is the starting point of the fitting procedure. The lower the noise of the data, the less ambiguous the choice of parameter values and their interpretation.

Equation (12) offers the possibility of deriving physical information from experimental data. The shape of the fitted curve can be connected to the physical parameters k_n, s_n, and the schedule of the experiment. The selection of the values for the parameters is not trivial. For instance, the schedule can be assumed as strictly fixed parameters or variables. The latter is appropriate if there is a time delay between cause and effect or if the events cannot be related to a known event from the schedule of the experiment.

3.2.2. Fitting Process for Phases with Active Source ($s_n >> 0$)

The source term s can be assumed as a variable or fixed value. If the curvature of the curve can be identified clearly, the parameter k_n is specified, and the connected source term s_n has to be calculated by Equation (14):

$$s_n = k_n \times \frac{c_n - c_{(n-1)} \times e^{-k_n \times (t_n - t_{(n-1)})}}{1 - e^{-k_n \times (t_n - t_{(n-1)})}} \quad (14)$$

where s_n is the source term in [µg/(m^3 h)] during phase n, k_n is the total loss coefficient in [h^{-1}] in phase n, c_n is the concentration in [µg/m^3] at the end of phase n at t_n in [h], and c_{n-1} is the concentration in [µg/m^3] at the beginning of phase n at t_{n-1} in [h].

On the other hand, if k_n cannot be specified adequately in a certain phase n due to high data noise, the source term s_n can be assumed as a constant parameter during several phases. In this case, the source term s_n is set equal to the source term of another phase in which the parameter k_n can be determined more adequately.

3.2.3. Fitting Process for Exponential Decay until Background Concentration Is Reached

Suppose the source is off and the concentration at the end of phase n is the background concentration. In this case, Equation (15) is used, and the parameter k_n is adjusted until the fitting curve meets the experimental data:

$$c_n(t) = c_0 + (c_{n-1} - c_0) \times e^{-k_n \times (t - t_{n-1})} \quad (15)$$

where $c_n(t)$ is the concentration in [µg/m^3] at a certain time t in [h], c_0 ($c_0 = c_n$) is the background concentration in [µg/m^3], c_{n-1} is the concentration in [µg/m^3] at the beginning of phase n at t_{n-1} in [h], and k_n is the total loss coefficient in [h^{-1}] in phase n.

The parameter s_n is calculated subsequently by Equation (16):

$$s_n = k_n \times c_0 \quad (16)$$

where s_n is the source term in [µg/(m^3 h)] in phase n, k_n is the total loss coefficient in [h^{-1}] in phase n, and c_0 ($c_0 = c_n$) is the background concentration in [µg/m^3].

3.2.4. Fitting Process for Exponential Decay If the Concentration at the End of the Phase Is Higher Than the Background Concentration

Suppose the source is off and the concentration at the end of phase n is higher than the background concentration c_0 ($c_n > c_0$). In this case, the parameter k_n is calculated by Equation (17):

$$k_n = ln\left(\frac{c_{n-1} - c_0}{c_n - c_0}\right) / (t_n - t_{n-1}) \quad (17)$$

where k_n is the total loss coefficient in [h^{-1}] in phase n, c_{n-1} is the concentration in [$\mu g/m^3$] at the beginning of phase n at t_{n-1} in [h], c_0 ($c_n > c_0$) is the background concentration in [$\mu g/m^3$], and c_n is the concentration in [$\mu g/m^3$] at the end of phase n at t_n in [h].

The parameter s_n is calculated subsequently by Equation (16).

3.2.5. Implementation of the Adjustment of the Parameters k_n and s_n

In a phase n without an active source ($s_n \cong 0$), the parameter k_n was calculated in Equation (17) or Equation (15), and the parameter s_n was calculated subsequently by Equation (16). The adjustable parameters were the concentrations c_{n-1} and c_n at the beginning (t_{n-1}) and the end (t_n) of phase n. In this case, the parameters k_n and s_n were unambiguous to a large extent (variance usually less than 5% and up to 10%).

The parameter k_n was the preferred fitting parameter also in phases with an active source ($s_n >> 0$). The exponential coefficient k_n was used to adjust the curvature of the fitting curve to the experimental data, while the parameter s_n was fixed using Equation (14).

When the noise of the experimental data was too high to specify k_n clearly in a certain phase n, the assumption of a constant source term was used to reduce the ambiguity. In this case, a phase $n = ref$ with a clearly specified k_{ref} (well-defined curvature) was selected as a reference for the value of s_{ref}, and the parameter k_n was changed until s_n equals s_{ref}. As a result, the parameter s_n was calculated by Equation (14).

3.2.6. Fitting Results

Figure 4a illustrates the fitting curve and the experimental data for the concentration at position 1 in the aircraft cabin close to the aerosol release. Figure 4b presents the trends of the parameters s_n and k_n at position 1, and the specific values can be extracted from Table 5. During the aerosol release, the total loss coefficient k_n amounted to about 17 h^{-1} and the source term about 4420 ($\mu g/m^3$)/h. When the aerosol release terminated, the loss coefficient k_n initially increased for a short moment and afterward decreased in several steps from 28.3 down to 3.9 h^{-1}. This result clearly indicates that the exponential decay coefficient is not constant over time. With the beginning of the pressure rise at 285 min, the coefficient k_n increased again due to venting the cabin with fresh air.

At position 2 (Figure 5a) and especially at position 3 (Figure 5b), the particle concentration is smaller than at position 1 due to the larger distance from the aerosol source. While the change of the cleaning technique from HEPA filter to non-thermal plasma almost did not affect the concentration at position 1 and slightly at position 2, the concentration at position 3 increased by a factor of about 3. This is a clear indication that the purification effect of the cleaning technique depends on location in the aircraft cabin.

Figure 6 illustrates the trends of k_n and s_n at positions 2 and 3. Several changes of k_n can be dedicated to events of the experimental schedule, like switching the aerosol release on and off, changing the cleaning technology, and the start of the pressure rise due to venting the aircraft cabin. The concentration drops and the increase of k_n at positions 2 and 3 at about 123 min and 225 min (Table 6) correlated with the beginning of the air sampling for bacteriophage plaque assays. The volume flow of the sampling pumps was 3 m^3/h and, therefore, in the range of typical respiratory flow volumes of approximately six passengers (0.5 m^3/h per person). The reason for the lower source term s_n during phases 1 and 2 at position 3 is unknown (194 instead of 524 ($\mu g/m^3$)/h). Due to the low noise in phase 2, the variance of parameter k_2 is low.

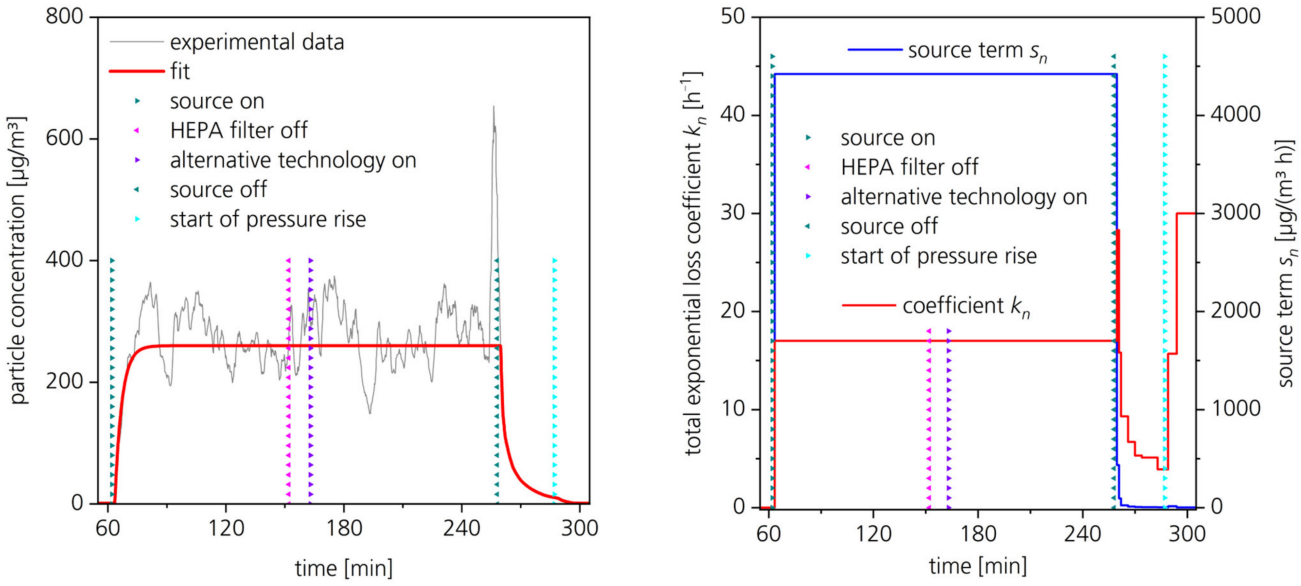

(**a**) (**b**)

Figure 4. Results of the particle measurement and fitting process at position 1 close to the aerosol release and the changed parameters like source on/off, start of pressure rise, and change of air cleaning technique and: (**a**) $PM_{2.5}$ and corresponding fitting curve; (**b**) parameters k_n and s_n of the fitting curve.

Table 5. Fitting parameters k_n and s_n for the fitting curve for position 1 and derived concentration $c_{start,n}$ at the beginning of phase n and equilibrium concentration $c_{eq,n}$.

Position in Cabin	Phase n * [-]	t_n (Start) # [min]	k_n [h^{-1}]	Uncertainty Factor of k_n	s_n [(µg/m³)/h]	Uncertainty Factor of s_n	$c_{start,n}$ [µg/m³]	$c_{eq,n}$ [µg/m³]
Position 1	1	63.5	17.0	1.4	4420	1.4	1.0	260
	2	259.7	28.3	1.1	435	2.0	260	9.2
	3	260.9	15.8	1.05	94	2.0	148	3.5
	4	262	9.3	1.05	23	2.0	111	2.4
	5	266	6.7	1.05	11	2.0	60.0	1.6
	6	270	5.3	1.05	7	2.0	38.8	1.3
	7	274	5.1	1.05	5	1.9	27.5	1.0
	8	283	3.9	1.05	4	1.7	13.4	1.0
	9	289	15.7	1.05	14	1.2	9.4	1.0
	10	294	30.0	1.05	2	1.2	3.4	0.4

* The fitted curve was divided into ten phases with individual fitting parameters k_n and s_n in each phase n. # The aerosol was generated between 62 min and 258 min while the pressure continuously was 750 hPa. Between 120 min and 150 min, as well as between 223 min and 253 min, microbiological sampling with 3 m^3/h proceeded. At 150 min, the HEPA filter was removed, and at 163 min, the alternative cleaning technology was built in. Venting the cabin started at 285 min.

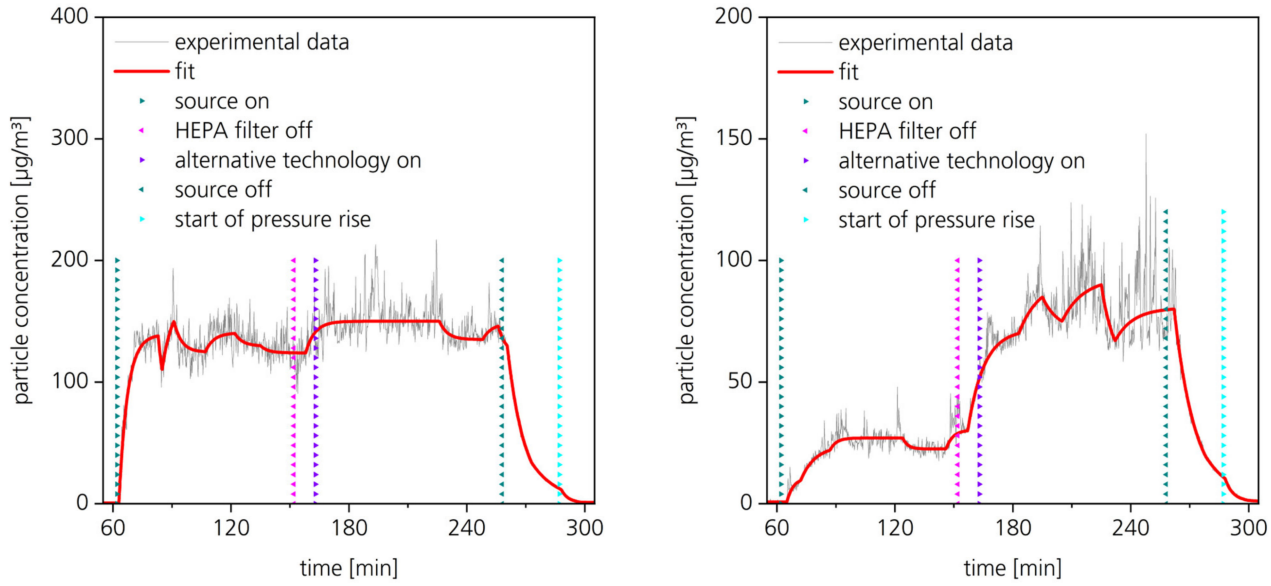

Figure 5. Experimental data of particle measurement (grey line) and fitted curve (red line) at positions in farther distance to the particle release: (**a**) $PM_{2.5}$ at position 2; (**b**) $PM_{2.5}$ at position 3.

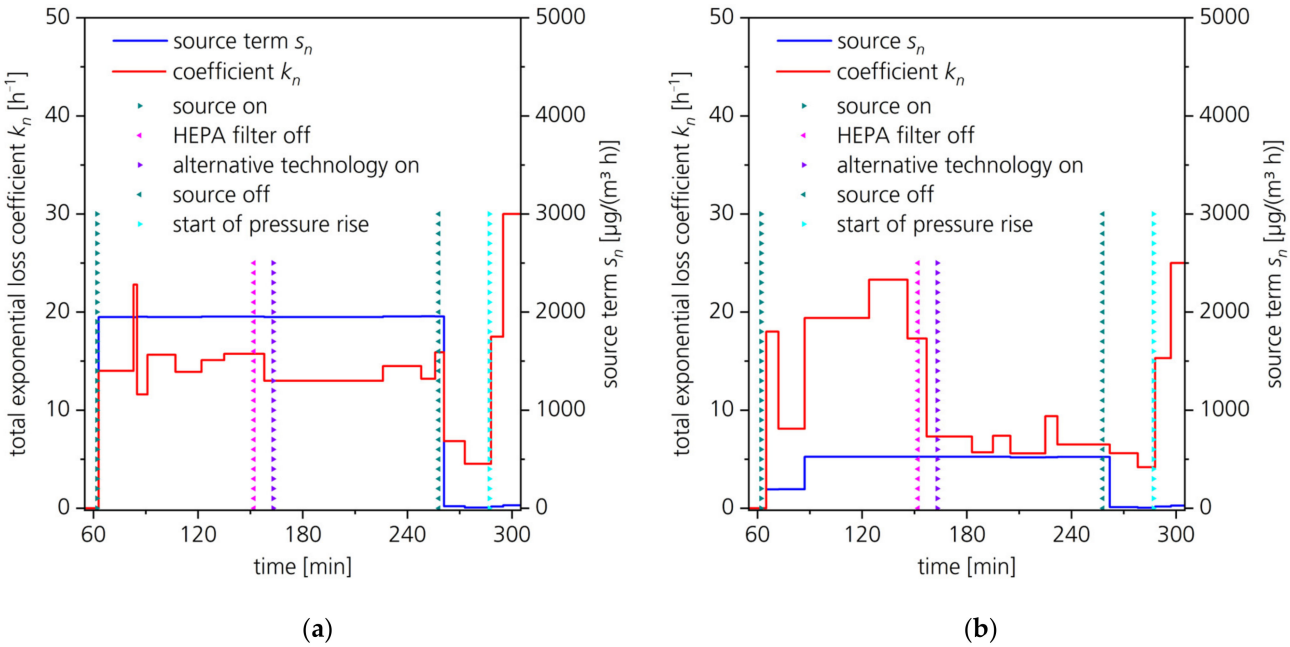

Figure 6. Fitted parameters k_n and s_n and changed parameters like source on/off, start of pressure rise, and change of air cleaning technique: (**a**) k_n and s_n at position 2; (**b**) k_n and s_n at position 3.

Table 6. Fitting parameters k_n and s_n for the fitting curves for position 2 and position 3 and derived concentrations $c_{start,n}$ at the beginning of phase n and equilibrium concentrations $c_{eq,n}$. The bold type values were used for the initial determination of k_n. In the other phases, the assumption of a constant source term was applicated.

Position in Cabin	Phase n * [-]	t_n (Start) # [min]	k_n [h^{-1}]	Uncertainty Factor of k_n	s_n [(µg/m³)/h)]	Uncertainty Factor of s_n	$c_{start,n}$ [µg/m³]	$c_{eq,n}$ [µg/m³]
Position 2	1	**63**	**14.0**	1.5	**1950**	1.5	0.5	139
	2	83	22.8	2.0	1947	2.9	138	85.4
	3	85	11.6	2.0	1952	1.8	110	168
	4	91	15.65	2.0	1950	2.0	150	125
	5	107	13.9	2.0	1950	2.0	125	140
	6	122	15.1	2.0	1953	2.0	140	129
	7	135	15.75	2.0	1953	2.0	130	124
	8	158	13.0	2.0	1950	2.0	124	150
	9	226	14.5	2.0	1956	2.0	150	135
	10	248	13.2	2.0	1957	2.0	135	148
	11	256	15.9	2.0	1956	2.2	146	123
	12	261	6.84	1.1	21	2.0	130	3.1
	13	273	4.53	1.1	6	2.0	32	1.3
	14	288	17.5	1.1	17	1.4	11	1.0
	15	295	30.0	1.1	30	1.0	2.3	1.0
Position 3	1	65	18.0	2.0	193	1.7	0.7	10.7
	2	**72**	**8.1**	**1.4**	**194**	1.3	9.5	23.9
	3	87	19.4	2.0	524	2.0	22.0	27.0
	4	124	23.3	2.0	524	2.0	27.0	22.5
	5	146	17.3	2.0	525	1.9	22.5	30.3
	6	**157**	**7.3**	**1.4**	**524**	1.4	30.0	71.8
	7	183	5.7	2.0	525	1.8	70.0	92.1
	8	195	7.4	2.0	525	2.2	85.0	70.9
	9	205	5.6	2.0	519	1.8	75.0	101.1
	10	225	9.4	2.0	521	2.4	94.0	61.1
	11	232	6.5	2.0	523	2.0	67.0	80.5
	12	262	5.61	1.1	12	2.0	81.0	2.1
	13	278	4.19	1.1	5	2.0	19.0	1.1
	14	288	15.3	1.1	17	1.2	10.0	1.1
	15	297	25.0	1.1	27	1.0	2.0	1.1

* Each fitted curve was divided into 15 phases with individual fitting parameters k_n and s_n in each phase n. # The aerosol was generated between 62 min and 258 min while the pressure was continuously 750 hPa. Between 120 min and 150 min, as well as between 223 min and 253 min, microbiological sampling with 3 m^3/h proceeded. At 150 min, the HEPA filter was removed, and at 163 min the alternative cleaning technology was built in. Venting the cabin started at 285 min.

4. Discussion

4.1. Case Study I: Determination of a Clean Air Delivery Rate under Well Mixed Conditions

Usually, testing procedures for determining a CADR utilize an exponential decay without continuous particle release and hence without a source term [2,4–7]. Schumacher et al. presented an equation analogous to Equation (5). However, they did not utilize their model to analyze experimental data [3]. No CADR evaluation method considering an aerosol release during the testing period could be found in the literature besides the utilization of the presented model for the analysis of particulate matter and bacteriophage plaque assays by Burdack-Freitag et al. and Schmohl et al. [13,23].

With the presented test schedule in combination with the application of the presented incremental evaluation model, the clean air delivery rate could be determined accurately with about 5% of uncertainty. Additionally, this method is very robust because the fitting is done over a long period. Therefore, short-term artifacts do not influence the result (e.g., Figure 3, PM_{10} at 1.5 h). Furthermore, a continuous aerosol release is more realistic than tests without aerosol release during the testing of the air cleaner.

The particle size distribution of the used aerosol and the particle size dependency of the filter efficiency have to be considered to determine a CADR [2,3,6]. In this research, this aspect was neglected to reduce the complexity of the topic.

The purpose of case study I was to validate the incremental evaluation model under controlled experimental conditions and to demonstrate the excellent agreement of the mathematical model with the experimental data.

4.2. Case Study II: Investigation of an Air Cleaner in an Aircraft Cabin

Computer-assisted simulations are commonly used to compare experimental data with calculated data [28,29]. Numerical simulations can provide spatial and temporal resolved parameters in high resolution. However, the effort to create a numerical simulation model is much higher than the utilization of the presented incremental evaluation model.

Usually, the effectiveness of air purification is investigated by a test setup that reduces the complexity of the system. For instance, a single-pass collection effectiveness assessment can be used, and the concentration before and after the cleaning device can be compared [9]. However, due to this simplification, the influence of the distance neither to the particle source nor to the air inlets and outlets can be determined. Case study II provides the first experimentally derived spatial and temporal resolved source terms s and total loss coefficients k in an aircraft cabin, thus under complex flow conditions.

Jung utilized an equation similar to Equation (12) to describe the change of CO_2 concentration in a car cabin [12]. However, no analysis with several time segments was executed.

The determined source terms in case study II were not equal to the release rate at Sheffield's head because only a part of the released particles reached the volume compartment where the aerosol spectrometers measured the particle concentration. The further the position of the aerosol spectrometer from Sheffield's head, the lower the source term. The realized source term in the volume compartment depends on flow characteristics. Therefore, a change in flow directions, for example, due to moving staff, can change the source term at a certain position. The assumption of a constant source term was used to reduce the complexity of the model. This can imply a shortcoming for the application of the incremental model. The set of parameters has to be plausible concerning the events and effects during the experiment.

Usual exponential decay models with a constant total loss coefficient were unsuitable for describing the concentration decay process after the aerosol release terminated. However, the presented incremental model could quantify the change of the total loss coefficient and the source term during the concentration decrease. At position 1, terminating the aerosol release resulted in a short increase of k_n (up to 28.3 h^{-1}) followed by a stabilization close to the k_n (approx. 5 h^{-1}) of positions 2 and 3. Physically, this indicates that the aerosol release in the proximity dominated and outperformed the benefit of the cleaning technology. Once the emission is terminated, the local particle cloud quickly dilutes until the concentration is homogeneous in the aircraft cabin (approx. 10 $\mu g/m^3$ at 288 min). The results for all three positions indicate a slowdown of particle loss after the aerosol release terminated. Initially, the particle diffusion effect contributed to the particle loss resulting in a high total loss coefficient. Afterwards, the loss process was increasingly dominated by the air exchange. At all three positions, the following increase of particle loss at approx. 288 min correlated with the pressure rise while venting the cabin.

Compared with the mean air exchange of 7.9 h^{-1}, the determined total loss coefficients were higher at all three positions (13–23 h^{-1}) while the HEPA filter was used. With the non-thermal plasma cleaning technique, the total loss coefficient was in the same range at positions 1 and 2, but at position 3, the total loss coefficient dropped to approximately 7 h^{-1}. The change of the total loss coefficient k during the experiment indicated whether the sampling position was affected mainly by the aerosol release or the air cleaning technology. The change of the cleaning technology resulted in a reduced total loss coefficient at position 3 (from 17.3 to 7.3 h^{-1}). On the contrary, the change did not affect the total loss coefficient at position 1 (17.0 h^{-1} constantly). This interpretation is consistent with the

higher source term s at position 1 (4420 (µg/m^3)/h) in comparison with position 3 (approx. 520 (µg/m^3)/h). These results confirmed the interpretation that the aerosol release in the proximity of the particle releasing source dominated and outperformed the benefit of the cleaning technology and that the particle diffusion effect contributed to the particle loss.

Additionally, the influence of a parallel air sampling for phage plaque assay could be quantified using the incremental model. The sampling resulted in an increase in the total loss coefficient at positions 2 (9–20%) and 3 (12–68%). An alternative set of parameters could be a stable loss coefficient combined with a reduced source term, but this option was assumed to be less plausible. The influence of parallel sampling should be considered in future investigations.

5. Conclusions and Outlook

5.1. Case Study I: Determination of a Clean Air Delivery Rate under Well Mixed Conditions

In realistic air cleaner applications, the source releases aerosol simultaneously while the air cleaner is purifying the indoor air without the support of external mixing, e.g., by fans. Air cleaners should be tested under similar conditions. Therefore, the testing procedure described in Table 7 is recommended for evaluating air cleaners.

Table 7. Recommended testing procedure for the evaluation of air cleaners.

Phase n	t_{start} [h]	Aerosol Release	Air Cleaner	Both Fans	Purpose
1	0.0	on	off	on	determination of $k_{nat,start}$ under ideal, well-mixed conditions
2	1.00	on	on	on	2 & 3: determination of $k_{AC,ideal}$ under ideal, well-mixed conditions
3	1.67	off	on	on	
4	2.33	on	on	off	4 & 5: determination of $k_{AC,real}$ under realistic conditions
5	3.00	off	on	off	
6	3.67	on	off	on	proof of stable aerosol generation by comparison with phase 1
7	4.33 *	off	off	on	proof of stable k_{nat} by comparison of $k_{nat,end}$ (n = 7) with $k_{nat,start}$ (n = 1)

* End of phase 7 at 5.00 h.

With the suggested testing procedure, it can be proved that the air cleaner can mix the air in the test room independently of the external air mixing devices during phases 4 and 5 (fan off). Subsequently, the last two phases can be applied to prove the stability of the aerosol generation (step 6, in combination with k_{nat} from step 7) and the natural loss coefficient k_{nat} (step 7).

In phases 4 and 5, the well-mixed condition is potentially not fulfilled. For these two phases, the data can be evaluated by the incremental model analogous to the scenario in the aircraft cabin (case study II).

5.2. Case Study II: Investigation of an Air Cleaner in an Aircraft Cabin

Spatial and temporal resolved source terms s and total loss coefficients k could be derived from the available experimental data. Thus, the local effectiveness of the air cleaning technology could be evaluated more reliably than without the application of the incremental evaluation model. Likewise, identifying some disturbance factors was possible (e.g., the effect of parallel air sampling on the total loss coefficient k or change of the source term s at position 3 at 87 min).

5.3. Applications beyond the Presented Case Studies

The presented model is limited to scenarios with zero-order and first-order kinetics processes. An adaptation of the equation is potentially needed if processes with second-order kinetics, such as chemical reactions of two air components, have to be considered. The effects independent of the concentration (=zero-order kinetics) affect the source term s, and the effects with first-order kinetics concerning the concentration affect the total loss coefficient k. The individual effects contributing to the source term s and the total loss

coefficient k have to be determined by a suitable design of the experiment, such as changing between periods with and without the purifying technology (or source, respectively). Additionally, the model could be extended with a release rate as a function of time.

With the incremental fitting model, even complex and challenging experiments with dynamic conditions can be described. The practical benefits are:

- Spatial and temporal resolved quantification of source terms s and total loss coefficients k;
- More reliable evaluation of the local effectiveness of an air purifying technology;
- Support in the identification of disturbance factors;
- Determination of the spatial and temporal resolved air exchange rate in indoor spaces, e.g., by a parallel controlled release of CO_2;
- Assistance in the planning of experiments through the prediction of expected matter concentrations and necessary sampling volumes (analogous to Schumacher et al. [3]).

Usually, the incremental evaluation model can be used independently from the kind of matter. For example, concentration curves of volatile organic compounds (VOC), CO_2 [12], N_2O [15], NO_2, NO, and Ozone [13] can also be analyzed. For instance, Jung utilized an equation analogous to Equation (12) to determine the evolution of the CO_2 concentration in car cabins, but without changing the experimental conditions and hence not as an incremental model [12]. Furthermore, the analysis of bioaerosols using plaque assays is feasible [13,23]. In the case of using air samples, such as for bacteriophage plaque assays, the integral of Equation (12) is needed [23]. Further investigations to evaluate the robustness of this tool are necessary and should proceed in future research. An objective and future topic is the transfer of the equations into a comfortably manageable evaluation tool.

Author Contributions: Conceptualization, A.S.; methodology, A.S., V.N. and M.B.; software, A.S.; validation, A.S., M.B. and V.N.; formal analysis, A.S.; investigation, M.B. and V.N.; resources, V.N. and M.B.; data curation, A.S. and M.B.; writing—original draft preparation, A.S. and M.B.; writing—review and editing, A.S., M.B., V.N., C.R.S., P.A.V.G. and C.S.; visualization, A.S. and M.B.; supervision, V.N. and S.J.; project administration, V.N. and S.J.; funding acquisition, V.N. and A.B.-F. All authors have read and agreed to the published version of the manuscript.

Funding: This research was funded by the Bavarian Ministry of Economic Affairs, Regional Development and Energy, aviation research program BayLu25, grant number ROB-2-3410.20_04-10-33/BLU-2109-0033.

Institutional Review Board Statement: Not applicable.

Informed Consent Statement: Not applicable.

Data Availability Statement: The data set is available from the corresponding author upon reasonable request.

Conflicts of Interest: The authors declare no conflict of interest. The funders had no role in the design of the study, in the collection, analyses, or interpretation of data, in the writing of the manuscript, or in the decision to publish the results.

References

1. Curtius, J.; Granzin, M.; Schrod, J. Testing mobile air purifiers in a school classroom: Reducing the airborne transmission risk for SARS-CoV-2. *Aerosol Sci. Technol.* **2021**, *55*, 586–599. [CrossRef]
2. Küpper, M.; Asbach, C.; Schneiderwind, U.; Finger, H.; Spiegelhoff, D.; Schumacher, S. Testing of an Indoor Air Cleaner for Particulate Pollutants under Realistic Conditions in an Office Room. *Aerosol Air Qual. Res.* **2019**, *19*, 1655–1665. [CrossRef]
3. Schumacher, S.; Asbach, C.; Schmid, H.-J. Effektivität von Luftreinigern zur Reduzierung des COVID-19-Infektionsrisikos/Efficacy of air purifiers in reducing the risk of COVID-19 infections. *Gefahrstoffe* **2021**, *81*, 16–28. [CrossRef]
4. *ANSI/AHAM AC-1-2020*; Method for Measuring Performance of Portable Household Electric Room Air Cleaners. Association of Home Appliance Manufacturers: Washington, DC, USA, 2020.
5. *GB/T 18801-2015*; Air Cleaner (Translated English version of Chinese National Standard). National Standard of the People's Republic of China: Beijing, China, 2016.
6. Wood, J. *Evaluation of In-Room Particulate Matter Air Filtration Devices*; EPA/600/R-08/012; Environmental Protection Agency: Washington, DC, USA, 2008; pp. 1–56.

7. *VDI-EE 4300 Blatt 14:2021-09*; Measurement of Indoor Pollution—Requirements for Mobile Air Purifiers to Reduce Aerosol-Borne Transmission of Infectious Diseases. Verein Deutscher Ingenieure e.V.: Düsseldorf, Germany, 2021.
8. Mølgaard, B.; Koivisto, A.J.; Hussein, T.; Hämeri, K. A New Clean Air Delivery Rate Test Applied to Five Portable Indoor Air Cleaners. *Aerosol Sci. Technol.* **2014**, *48*, 409–417. [CrossRef]
9. Pellegrin, B.; Berne, P.; Giraud, H.; Roussey, A. Exploring the potential of electrostatic precipitation as an alternative particulate matter filtration system in aircraft cabins. *Indoor Air* **2022**, *32*, e12990. [CrossRef] [PubMed]
10. Reed, C.; Nabinger, S.J.; Emmerich, S.J. Measurement and simulation of the indoor air quality impact of gaseous air cleaners in a test house. *Proc. Indoor Air* **2002**, *2*, 652–657.
11. Chan, W.R.; Logue, J.M.; Wu, X.; Klepeis, N.E.; Fisk, W.J.; Noris, F.; Singer, B.C. Quantifying fine particle emission events from time-resolved measurements: Method description and application to 18 California low-income apartments. *Indoor Air* **2018**, *28*, 89–101. [CrossRef] [PubMed]
12. Jung, H. *Modeling CO_2 Concentrations in Vehicle Cabin*; SAE Technical Paper 2013-01-1497; SAE International: Warrendale, PA, USA, 2013; pp. 1–6. [CrossRef]
13. Burdack-Freitag, A.; Buschhaus, M.; Grün, G.; Hofbauer, W.K.; Johann, S.; Nagele-Renzl, A.M.; Schmohl, A.; Scherer, C.R. Particulate Matter versus Airborne Viruses—Distinctive Differences between Filtering and Inactivating Air Cleaning Technologies. *Atmosphere* **2022**, *13*, 1575. [CrossRef]
14. Manoukian, A.; Quivet, E.; Temime-Roussel, B.; Nicolas, M.; Maupetit, F.; Wortham, H. Emission characteristics of air pollutants from incense and candle burning in indoor atmospheres. *Environ. Sci. Pollut. Res.* **2013**, *20*, 4659–4670. [CrossRef]
15. Bivolarova, M.; Ondráček, J.; Melikov, A.; Ždímal, V. A comparison between tracer gas and aerosol particles distribution indoors: The impact of ventilation rate, interaction of airflows, and presence of objects. *Indoor Air* **2017**, *27*, 1201–1212. [CrossRef] [PubMed]
16. Nazaroff, W.W.; Cass, G.R. Mathematical modeling of indoor aerosol dynamics. *Environ. Sci. Technol.* **1989**, *23*, 157–166. [CrossRef]
17. Nazaroff, W.W. Indoor particle dynamics. *Indoor Air* **2004**, *14*, 175–183. Available online: https://escholarship.org/uc/item/7sq4x34d (accessed on 29 August 2022). [CrossRef] [PubMed]
18. Nazaroff, W.W. Indoor bioaerosol dynamics. *Indoor Air* **2016**, *26*, 61–78. [CrossRef] [PubMed]
19. Silcott, D.; Kinahan, S.; Santarpia, J. TRANSCOM/AMC Commercial Aircraft Cabin Aerosol Dispersion Tests. 2020. Available online: https://www.ustranscom.mil/cmd/docs/TRANSCOM%20Report%20Final.pdf (accessed on 29 August 2022).
20. Zee, M.; Davis, A.C.; Clark, A.D.; Wu, T.; Jones, S.P.; Waite, L.L.; Cummins, J.J.; Olson, N.A. Computational fluid dynamics modeling of cough transport in an aircraft cabin. *Sci. Rep.* **2021**, *11*, 23329. [CrossRef] [PubMed]
21. Matheis, C.; Norrefeldt, V.; Will, H.; Herrmann, T.; Noethlichs, B.; Eckhardt, M.; Stiebritz, A.; Jansson, M.; Schön, M. Modeling the Airborne Transmission of SARS-CoV-2 in Public Transport. *Atmosphere* **2022**, *13*, 389. [CrossRef]
22. Woodward, H.; Fan, S.; Bhagat, R.K.; Dadonau, M.; Wykes, M.D.; Martin, E.; Hama, S.; Tiwari, A.; Dalziel, S.B.; Jones, R.L.; et al. Air Flow Experiments on a Train Carriage—Towards Understanding the Risk of Airborne Transmission. *Atmosphere* **2021**, *12*, 1267. [CrossRef]
23. Schmohl, A.; Nagele-Renzl, A.M.; Buschhaus, M.; Johann, S.; Scherer, C.R.; Grün, G.; Hofbauer, W.K.; Burdack-Freitag, A. Determination of CADR of virus-inactivating air purifiers by surrogate virus plaque assay. In Proceedings of the Indoor Air 2022, 17th International Conference of the International Society of Indoor Air Quality & Climate, Kuopio, Finland, 12–16 June 2022; pp. 1–8.
24. *AHAM AC-5-2022*; Method for Assessing the Reduction Rate of Key Bioaerosols by Portable Air Cleaners Using an Aerobiology Test Chamber. Association of Home Appliance Manufacturers: Washington, DC, USA, 2022.
25. Baer, A.; Kehn-Hall, K. Viral concentration determination through plaque assays: Using traditional and novel overlay systems. *J. Vis. Exp.* **2014**, *93*, e52065. [CrossRef] [PubMed]
26. *DIN EN 13610:2003-06*; Chemische Desinfektionsmittel—Quantitativer Suspensionsversuch zur Bestimmung der Viruziden Wirkung Gegenüber Bakteriophagen von Chemischen Desinfektionsmitteln in den Bereichen Lebensmittel und Industrie—Prüfverfahren und Anforderungen (Phase 2, Stufe 1). Deutsche Fassung EN 13610:2003; Deutsches Institut für Normung e.V.: Berlin, Germany, 2003.
27. Norrefeldt, V.; Buschhaus, M.; Nagele-Renzl, A.M. European Patent Application: Aerosolgenerator und Verfahren zur Abgabe eines Aerosols. Patent Application No. 21212872.2, 7 December 2021.
28. Dbouk, T.; Roger, F.; Drikakis, D. Reducing indoor virus transmission using air purifiers. *Phys. Fluids* **2021**, *33*, 103301. [CrossRef] [PubMed]
29. Burgmann, S.; Janoske, U. Transmission and reduction of aerosols in classrooms using air purifier systems. *Phys. Fluids* **2021**, *33*, 033321. [CrossRef] [PubMed]